STEM CELLS AND DEVELOPMENT
Volume 25, Number 7, 2016

DOI: 10.1089/scd.2015.0321

The Universal 3D3 Antibody of Human PODXL Is Pluripotent Cytotoxic, and Identifies a Residual Population After Extended Differentiation of Pluripotent Stem Cells

Lei Kang,[1,2,*] Chunping Yao,[1–3,*] Alireza Khodadadi-Jamayran,[1,2] Weihua Xu,[1,2,4] Ruowen Zhang,[1,2] Nilam Sanjib Banerjee,[2] Chia-Wei Chang,[1,2] Louise T. Chow,[2] Tim Townes,[1,2] and Kejin Hu[1,2]

Abstract

Podocalyxin-like protein (PODXL) is a member of CD34 family proteins. It is the protein that carries many post-translational epitopes responsible for various pluripotent surface markers including TRA-1-60, TRA-1-81, GCTM2, GP200, and mAb84. However, PODXL has not attracted the attention of stem cell biologists. Here, we report several features of PODXL mRNA and protein in pluripotent stem cells. Similar to the modification-dependent pluripotent epitopes, PODXL transcripts and carrier protein are also features of pluripotency. PODXL is highly expressed in early human embryos from oocytes up to four-cell stages. During reprogramming of human cells to pluripotency, in contrast to TRA-1-60 and TRA-1-81, *PODXL* is activated by KLF4 at a very early time of reprogramming. Although TRA-1-60 and TRA-1-81 are completely lost upon differentiation, a residual PODXL$^+$ population exists even after extended differentiation and they were identified by the universal human PODXL epitope 3D3. Unlike TRA-1-60 and TRA-1-81 epitopes that are unique to primate pluripotent stem cells (PSCs), PODXL carrier protein can be used as a murine surface marker. Most importantly, antibody to 3D3 epitope causes massive necrosis and apoptosis of human PSCs (hPSCs). We suggest that 3D3 antibody could be employed to eliminate the tumorigenic pluripotent cells in hPSC-derived cells for cell transplantation.

Introduction

Human pluripotent stem cells (hPSCs) include human embryonic stem cells (hESCs) [1] and the man-made version human induced PSCs (HiPSCs) [2–5]. hPSCs are invaluable resources for basic research, regenerative medicine, and drug screening. hPSCs are governed by key transcriptional networks, in which OCT4, SOX2, and NANOG play a central role in the regulations of pluripotency and self renewal [6]. hPSCs are also defined by a set of surface markers, including ALP, SSEA3, SSEA4, SSEA5, TRA-1-60, TRA-1-81, and others [7–13]. In contrast to the intensely studied pluripotency-defining transcription factors, little is known about these pluripotent surface markers. Among these surface markers, TRA-1-60 and TRA-1-81 represent two distinct epitopes from the same carrier protein, podocalyxin-like protein (PODXL) [8,10]. PODXL is also the protein that carries epitopes for other less known pluripotent surface makers, such as GCTM2, GP200, and mAb84 [14,15]. As markers, they are lost upon differentiation of hPSCs. These antibody-defined epitopes represent distinct post-translational modifications, whereas the 3D3 antibody defines a PODXL epitope devoid of post-translational modifications because the antigen fragment was produced in bacteria and 3D3 was successfully used to detect various PODXL glycoforms [16]. It is widely thought that these PODXL markers are not shared with mouse pluripotent stem cells.

PODXL is a member of the CD34 family, which also includes CD34 and endoglycan. PODXL is an integral transmembrane protein heavily modified with O-glycosylation, N-glycosylation, sialylation, and sulfation [17]. It is highly expressed in kidney epithelium, and it is also expressed in several other cell types, including hematopoietic progenitors, endothelium, platelets, and some neural cells. Its well-known

[1]Stem Cell Institute, Department of Biochemistry and Molecular Genetics, University of Alabama at Birmingham, Birmingham, Alabama.
[2]Department of Biochemistry and Molecular Genetics, University of Alabama at Birmingham, Birmingham, Alabama.
[3]Department of Radiation Oncology, Shandong Cancer Hospital & Institute, Jinan, China.
[4]Longyan University, Fujian, China.
*These two authors contributed equally to this work.

role is in the development of kidney epithelia and maintenance of the podocyte filtration slit. PODXL knockout mice die within 24 h after birth due to anuria [18]. It plays various roles in different cells including antiadhesion, adhesion, cell matrix interaction, morphogenesis, and cell signaling. It is also associated with more than 10 human malignancies [15,19–25]. However, PODXL receives little attention in the field of pluripotent stem cells although numerous pluripotent surface markers are associated with it.

Here, we report several characteristics of PODXL in the context of hPSCs: (a) not only the post-translational modifications are a human pluripotent feature, PODXL is also a general pluripotent marker; (b) PODXL is a mouse ESC marker as well although its modification-dependent epitopes are not shared between human and mouse; (c) KLF4 activated *PODXL* at an early stage of reprogramming; (d) 3D3, a universal antibody of PODXL, identifies a residual $PODXL^+$ population after differentiation of hPSCs, whereas other modification-dependent PODXL antibodies failed to do so; (e) the antibody 3D3 is cytotoxic to human pluripotent stem cells.

Materials and Methods

Cell culture and reprogramming

Lenti-X 293T (#632180; Clontech) and Hela cells were maintained in DMEM medium supplemented with 10% heat-inactivated fetal bovine serum (FBS), 100 U/mL penicillin and 100 μg/mL streptomycin, and 0.1 mM MEM NEAA. Human fibroblasts (BJ: ATCC CRL-2522™) were cultured in fibroblast medium: DMEM (#12800-058; Gibco) supplemented with 10% heat-inactivated FBS (#10437; Gibco), 0.1 mM 2-mercaptoethanol (#194834; MP), 100 U/mL penicillin and 100 μg/mL streptomycin (#15140-122; Gibco), 0.1 mM MEM NEAA (#11140-050; Gibco), and 4 ng/mL human FGF2 (Nacalai USA, NU0005-**6**).

For reprogramming, BJ cells were seeded into 24-well plates at 2.0×10^4 cells/well. To determine the multiplicity of infection (MOI) for BJ transduction, cells from a spare well were counted 24 h postplating. The amount of viruses for the reprogramming factors is OCT4, 10 MOI; SOX2, 5 MOI; and KLF4, 5 MOI. Cells were transduced in the presence of 6 μg/mL hexadimethrine bromide (#107689; Sigma). Viruses were removed by medium change after overnight incubation. Cells were reseeded into Matrigel (A1413302; Geltrex)-coated 6-well plates 48 h post virus transduction in 1:10 to 1:12 ratio. Reprogramming was conducted in E7 medium: DMEM/F12 (#12400-024; Gibco) supplemented with 64 mg/L L-ascorbic acid 2-phosphate sesquimagnesium (A8690; Sigma), 13.6 μg/L sodium selenium (S5261; Sigma), 1.7 g/L $NaHCO_3$ (BP328-1; Fisher Scientific), 1 g/L sodium chloride (BP358-10; Fisher Scientific), 10 ng/mL FGF2, 20 μg/mL insulin (I2643; Sigma), and 10 μg/mL holotransferrin (T0665; Sigma) every day from day 3–13 post virus transduction. E8 medium (E7 + 2 μg/L TGFβ1 [8915LC; Cell Signaling]) was used from day 14–21.

Human ESCs (H1 and H9, WiCell, Wisconsin) and human iPSCs (3RiPSC2, 3RiPSC3, 3RiPSC4, and CD34iPSC6, generated in our lab) were maintained in E8 medium. Mouse ESCs (E14) were cultured in mouse ES cell growth medium: Knockout DMEM (#10829; Invitrogen) supplemented with 15% ES-certified FBS (#10439; Invitrogen), 2 mM L-glutamine (#21051-024; Gibco), 0.1 mM MEM NEAA, 0.5% COS-LIF supernatant medium, and 0.1 mM 2-mercaptoethanol.

Lentivirus packaging, concentration, and titration

Lenti-X 293T cells were seeded in 15-cm dishes at a density of 1.0×10^7 cells/dish 24 h before transfection. When cells reached ~70–80% confluence, medium was refreshed 1 h before transfection. A total of 60 μg of plasmid DNA (30 μg transfer plasmid, 10.5 μg envelop plasmid pMD2-G, and 19.5 μg packaging plasmid ps-PAX2) was mixed with 150 μL of 0.25 M calcium chloride and 1.35 mL sterilized HPLC water. The DNA-calcium solution was further mixed with equal volume of 2× HBS (pH 7.05). Formation of DNA-calcium phosphate complexes was facilitated by vortexing for 20 s before adding into the dish. The transfection culture medium was changed with fresh fibroblast medium 16 h post-tranfection. Viruses were collected between 48 and 72 h post-transfection. Cell debris was removed from the virus-containing medium at 3,000 *g* for 10 min at 4°C followed by filtration through a 0.45-μm filter (SCHVU01RE; Millipore). Lentivirus was precipitated with 8.5% PEG-6000 (final concentration, from 50% stock) (5288771KG; Millipore) and 0.4 M sodium chloride in a 50-mL tube for 3–5 h at 4°C. Virus pellet was obtained by centrifugation at 4,000 *g* for 40 min at 4°C, which was consecutively resuspended in 50 mM Tris-HCl (pH 7.4) with a concentration ratio of around 100–150×. The concentrated virus stock was divided into small aliquot (20 μL), and kept in −80°C. Viral titer was determined with flow cytometry for the expression of GFP in virus-transduced Hela cells.

Plasmid construction, transient transfection, and luciferase assay

PODXL promoter region (−2198 to −163) was amplified from genomic DNA of hiPS cell lines using forward primer (PODXL-PROM3-F): 5′-CCAGCCTCATTCCAGAAAGC and reverse primer (PODXL-PROM3-R): 5′-GCCGTGAA CAATGAGCAGAG. The PCR fragment was inserted into Sma I site of pGL3-Basic vector (E1751; Promega) to generate P2K plasmid. A shorter P0.5K plasmid was constructed by amplifying PODXL promoter region (−500 to −163) from P2K using forward primer (pPODXL-0.5k.F): 5 ′-TCAACGC GTGGGAGATGAGCTTCTCCG and reverse primer POD XL-PROM3-R. *PODXL* proximal promoter region (PODXL-TSS: −455 to −1/+1) was synthesized and cloned onto Sma I and Bgl II sites of pUC57 by Genewiz. Such fragment was double digested with Sma I and Bgl II and inserted into the previous intervening plasmids to generate pGL3-PODXL.500 and pGL3-PODXL.2198 plasmids; Plasmids overexpressing OCT4, SOX2, KLF4, and c-MYC under CMV promoter were constructed using PCR-amplified human cDNAs.

Hela cells were seeded in 24-well plates at a density of 5.0×10^4 cells/well 24 h before plasmid transfection. Cells were co-transfected with O/S/K/M (1 μg/well), *PODXL* promoter plasmids (pGL3-PODXL.500 or pGL3-PODXL.2198: 0.5 μg/well), and internal control plasmid pRL-TK (25 ng/well) using Lipofectamine 3000 (L3000; Invitrogen) per manufacturer's instructions. Luciferase assay was performed 48 h post-transfection with Dual-Luciferase Kit (E1910; Promega).

Western blotting

Whole cell lysates were prepared by rotating cells in RIPA buffer: 100 mM Tris-HCl (pH 7.4), 150 mM sodium chloride, 1 mM EDTA, 1% Triton-X-100, 1% sodium deoxycholate, 0.1% sodium dodecyl sulfate (SDS), and 1× Pierce Halt Protease Inhibitor cocktail (#78429; Pierce) for 30 min at 4°C. Proteins were fractionated on 7.5% SDS-PAGE, and transferred onto polyvinylidene difluoride membranes (#1602177; Bio-Rad). Membrane was blocked with 5% nonfat milk in TBS-T (0.2‰ Tween-20 in 1× Tris-buffered saline) for 45 min, and then was blotted for 2 h with primary antibodies: human PODXL (sc-23904, 3D3; Santa Cruz Biotech); mouse PODXL (AF1556; R&D); GAPDH (sc-25778; Santa Cruz Biotech); P21 (#2947, Cell Signaling), or β-actin (#4970; Cell Signaling). Membrane was further incubated with secondary antibodies: anti-mouse IgG-HRP (#7076; Cell Signaling), or anti-rabbit IgG-HRP (#7074; Cell Signaling). Protein blots were analyzed with Image Lab software on Bio-Rad ChemiDoc MP Imaging System.

Reverse transcription-quantitative polymerase chain reaction

Cells were lysed in TRIzol reagent (#15596-018; Invitrogen). Total RNAs were extracted using the Direct-zol™ RNA Miniprep Kit (R2052; Zymo Research). cDNAs were synthesized with M-MLV reverse transcriptase (#28025-013; Invitrogen). Quantitative PCR was performed in triplicates on ViiA 7 Real-time PCR system (Applied Biosystem) using SYBR-Green Master PCR mix (#639676; Clontech). Primers used for qPCR were listed in Supplementary Table S1 (Supplementary Data are available online at www.liebertpub.com/scd). Data were normalized to endogenous *GAPDH* for quantification.

Antibody treatment

Human pluripotent stem cells were seeded in 12-well plates at a density of 5.0×10^4 cells/well 24 h before antibody treatments. Cells were incubated with vehicle (0.1% sodium azide stock), control mouse IgG (10400C; Life Technologies), or different antibodies: SSEA-4 (MAB4304; Millipore), TRA-1-60 (MAB4360; Millipore), and PODXL (sc-23904; Santa Cruz Biotech or MABD89; Millipore) at a concentration of 1 μg per 1.0×10^5 cells, or 1–3 μg/mL. Cell numbers were counted every day using replicated wells of the same treatments as references to calculate the amount of antibodies to be added for each treatment on that day. Cell growth curve was generated for treatments for four continuous days, and fresh antibodies were added every 24 h together with daily medium change.

Embryoid body formation and in vitro differentiation

PSCs were grown to 70% confluence in six-well plates. Cells were collected and aggregated in AggreWell™ 400 plate (#27845; STEMCELL) per manufacturer's instructions. Cell aggregates were transferred to Ultra-Low Attachment Surface six-well plates (#3471; Corning) on day 4, and were further cultured in suspension for another 10 days before being seeded on 0.1% gelatin-coated six-well plates. Embryoid body (EB) differentiation was induced by FBS for more than 30 days. Culture medium was refreshed every other day, with the concentration of FBS increasing gradually from 2% to 10%.

Teratoma formation for in vivo differentiation

PSCs were grown to 70% confluence in six-well plates. Cells were harvested and divided into small aliquots (1.0×10^6 cells in 100 μL cold E8 medium supplemented with 30% Matrigel). Bilateral subcutaneous injection was performed on 6–8 week immunocompromised NSG mice. Teratoma was harvested 8 weeks after initial injection. UAB Institutional Animal Care and Use Committee approved the mouse procedure used in this study.

Flow cytometry

Harvested cells were resuspended in 1 mL fluorescence-activated cell sorting (FACS) buffer (2% BSA, 2 mM EDTA, and 0.05% sodium azide in PBS), and cell clumps were removed by a cell strainer. The individualized cells were collected by centrifugation. Cell pellet were resuspended in FACS buffer. About 2.0×10^5 cells in 100 μL FACS buffer were incubated with primary antibody at 4°C for 30 min. After washing cells with 3 mL FACS buffer, cells were further incubated with Alexa Fluor 488-labeled secondary antibody at 4°C for 30 min. The cells were then washed with 3 mL FACS buffer. Cell pellet was resuspended in 600 μL FACS buffer. Then, 10 μL 7-AAD (20 μg/mL stock) was added before assay with flow cytometer (LSRFortessa™; BD Bioscience). Antibodies used are hPODXL (sc-23904, 3D3; Santa Cruz Biotech) or mPODXL antibodies (AF1556; R&D), goat anti-mouse IgG (A10667; Invitrogen), Alexa Fluor 488-donkey anti-goat IgG (A11055; Invitrogen), PE-SSEA4 (#560128; BD Pharmingen), PE-TRA-1-60 (#560193; BD Pharmingen), or PE-SSEA1 (#560886; BD Pharmingen).

Apoptosis assay

Cellular apoptosis and necrosis were analyzed on flow cytometer using Annexin V PE Apoptosis Detection Kit (#88-8102; eBioscience) per manufacturer's instructions.

Chromatin Immunoprecipitation

Cells were collected and divided into aliquots (3–5 million) in 500 μL PBS. Then, 13.9 μL 37% formaldehyde (final concentration 1%) was added into the tube to cross-link DNA-protein for 8 min at RT. Formaldehyde was then quenched with 27 μL of 2.5 M glycine (final concentration 125 mM) for 5 min. Cells were collected by centrifugation at 500 *g* for 10 min. Cell pellet was then washed with 1 mL ice-cold hypotonic buffer (20 mM HEPES-KOH pH 7.5, 20 mM KCl, 1 mM EDTA, 10% glycerol, 1 mM DTT, 0.1 mM PMSF, and 1× Halt Protease Inhibitor cocktail). Washed cells were collected by centrifugation at 500 × *g* for 10 min. The cells undergo three rounds of freeze-thaw cycle between liquid nitrogen and RT. Cells were resuspended in 1 mL ice-cold lysis buffer (50 mM HEPES-KOH pH 7.5, 140 mM NaCl, 1 mM EDTA, 10% glycerol, 0.5% NP-40, 0.25% Triton-X-100, 1 mM DTT, 0.1 mM PMSF, and 1× Halt Protease Inhibitor cocktail). Cell suspension was rocked for 10 min at 4°C. Nuclei were collected by centrifugation at 750 *g* for 10 min at 4°C and washed with 1 mL ice-cold wash buffer (10 mM Tris-HCl pH 8.0, 200 mM NaCl, 1 mM EDTA, 0.5 mM EGTA, 1 mM DTT, 0.1 mM PMSF, and 1× Halt Protease Inhibitor cocktail). After wash, the nuclei were lysed for 30 min on ice in 300 μL sonication-lysis buffer

(10 mM Tris-HCl, pH 8.0, 100 mM NaCl, 1 mM EDTA, 0.5 mM EGTA, 0.1% sodium deoxycholate, 0.5% N-lauroylsarcosine, 1 mM DTT, 0.1 mM PMSF, and 1× Halt Protease Inhibitor cocktail). Chromatin sonication was then performed using diagenode bioruptor (3 × 10 cycles: 30 s ON/OFF). Sheared chromatin was collected by centrifugation at 14,000 *g* for 15 min at 4°C, and it was quantified using Nanodrop Spectrophotometer (Thermo Scientific).

For each chromatin immunoprecipitation (ChIP), 50 μL protein G beads slurry (#29398; Pierce) were washed thrice with 1 mL blocking buffer (0.5% BSA in 0.2‰ PBS-Tween). The beads were saturated with 10 μg HA antibody (Abcam, ab9110) or corresponding rabbit IgG control (ab37415; Abcam) in 1 mL blocking buffer by rotating at 4°C for 6 h. ChIP was performed by mixing 80 μg of sheared chromatin with antibody-beads and rotating for another 16 h at 4°C. The beads were transferred to fresh prechilled tubes and washed five times with 1 mL ice-cold Li-RIPA buffer (50 mM HEPES-KOH pH 7.5, 500 mM LiCl, 1 mM EDTA, 1% NP-40, and 0.7% sodium deoxycholate). The ChIP'd chromatin was eluted from beads with 200 μL elution buffer (50 mM Tris-HCl pH 8.0, 10 mM EDTA, and 1% SDS) by gentle agitation for 1 h at 65°C. Cross-linking of protein to chromatin was reversed by incubating the samples at 65°C for 18 h. Equal volume (200 μL) of TE buffer (10 mM Tris-HCl pH 8.0 and 1 mM EDTA) was added to the tube to dilute SDS. Proteinase K (0.2 mg/mL) treatment was carried out for 2 h at 55°C to digest any residual protein in the sample. DNA was purified using PureLink PCR Purification kit (K3100; Invitrogen) and resuspended in 50 μL TE buffer. DNA concentration was determined using Qubit fluorometer (Invitrogen).

RNA-Seq

mRNA-sequencing was performed on the Illumina HiSeq2500 using the sequencing reagents and flow cells providing up to 300 Gb of sequence information per flow cell. Briefly, the quality of the total RNA was assessed using the Agilent 2100 Bioanalyzer followed by two rounds of polyA+ selection and conversion to cDNA. We used the stranded mRNA library generation kits per manufacturer's instructions (Agilent). Library construction consists of random fragmentation of the polyA mRNA, followed by cDNA production using random primers with inclusion of actinomycin D in the first strand reaction. The ends of the cDNA are repaired, A-tailed and adaptors ligated for indexing (four different barcodes per lane) during the sequencing runs. The cDNA libraries were quantitated using qPCR in a Roche LightCycler 480 with the Kapa Biosystems kit for library quantitation (Kapa Biosystems) before cluster generation. Clusters were generated to yield ~725K–825K clusters/mm^2. Cluster density and quality were determined during the run after the first base addition parameters were assessed. We ran paired end 2 × 50 bp sequencing runs to align the cDNA sequences to the reference genome.

Bioinformatics

All the reads from our RNA-seq (GSE66798) [26] and the reads from the experiments GSE71645 [27], GSE59528 [28] and GSE36552 [47] were mapped to the human reference genome (GRCh37/hg19) using the STAR aligner [29] guided by a gene transfer file (Ensembl GTF version GRCh37.70).

Read count tables were generated using HTSeq (v0.6.0) [30] and were normalized based on their geometric library size factors. Deferential Expression (DE) analysis was performed using DESeq (v3.0) [31] due to its better performance than the widely used RPKM normalization [32].The Read Per Million (RPM) normalized BigWig files were generated using BEDTools (v2.17.0) [33] and bedGraphToBigWig tool (v4) [34]. For the DE analysis of the microarray data all the raw CEL files from GSE34200 were analyzed using the Limma R package (v3.0) [35]. All the downstream statistical analyses and data visualizations were performed in R (v3.1.1;http://www.r-project.org/).

Immunohistochemistry

Teratomas were fixed in formalin and were sectioned at UAB histology laboratory. Thin tissue sections (5 μm) are rehydrated and treated for heat-induced antigen retrieval in citrate buffer (pH 6.0). Tissue sections were treated with 3% hydrogen peroxide. They were probed with anti-PODXL (sc-23904, 3D3; Santa Cruz Biotech) and anti OCT4a (mouse, IgG2b, sc5279) overnight at 4°C per manufacturer protocol, followed by treatment with biotinylated anti mouse (A10519; IgG1, Invitrogen) and detected with streptavidine-HRP cy3-conjugated tyramide (SAT04A001EA; Perkin-Elmer). The same slides were again treated with 3% hydrogen peroxide and probed with hydroxyl peroxidase-conjugated anti-mouse IgG2b antibody followed by fluorescein-conjugated tyramide (Perkin Elmer NEL701001KT) to detect OCT4(a/b). Tissue sections were stained with DAPI (H1200; Vector). Images were captured using Olymous BX3 microscope with Olympus camera and software.

Results

High PODXL transcription is a signature of human pluripotent stem cells

PODXL encodes a protein that carries epitopes for several well-established hPSC markers including TRA-1-60, TRA-1-81, GP200, GCTM-2, and mAb84 [8,15,36]. These marker antibodies recognize epitopes of distinct post-translational modifications. It is possible that only the differential post-translational modifications are features of pluripotency considering the extensive and cell type-specific protein modifications as shown by huge difference in the apparent molecular weights in western blots. Specifically, the calculated MW is 58 kD. In hPSCs and somatic cells the protein has mobility around 200 kD, or 100–170 kD, respectively [16,37,38]. We asked whether the transcription of PODXL is characteristic of pluripotency. *PODXL* is among the lists of genes whose expression is elevated in human embryonic stem cells (hESC) based on several previous transcriptome profiling of hESCs using limited samples [39–43]. To address this question firmly, we analyzed a recent large pluripotent dataset GSE34200, which is a microarray transcription profiling of 21 hESC lines registered at NIH, 8 human iPSC lines and 20 human tissues [44]. Impressively, the expression of *PODXL* in hPSCs is higher than that of the housekeeping gene *GUSB*, and comparable to that of beta actin and GAPDH (Fig. 1A). Its

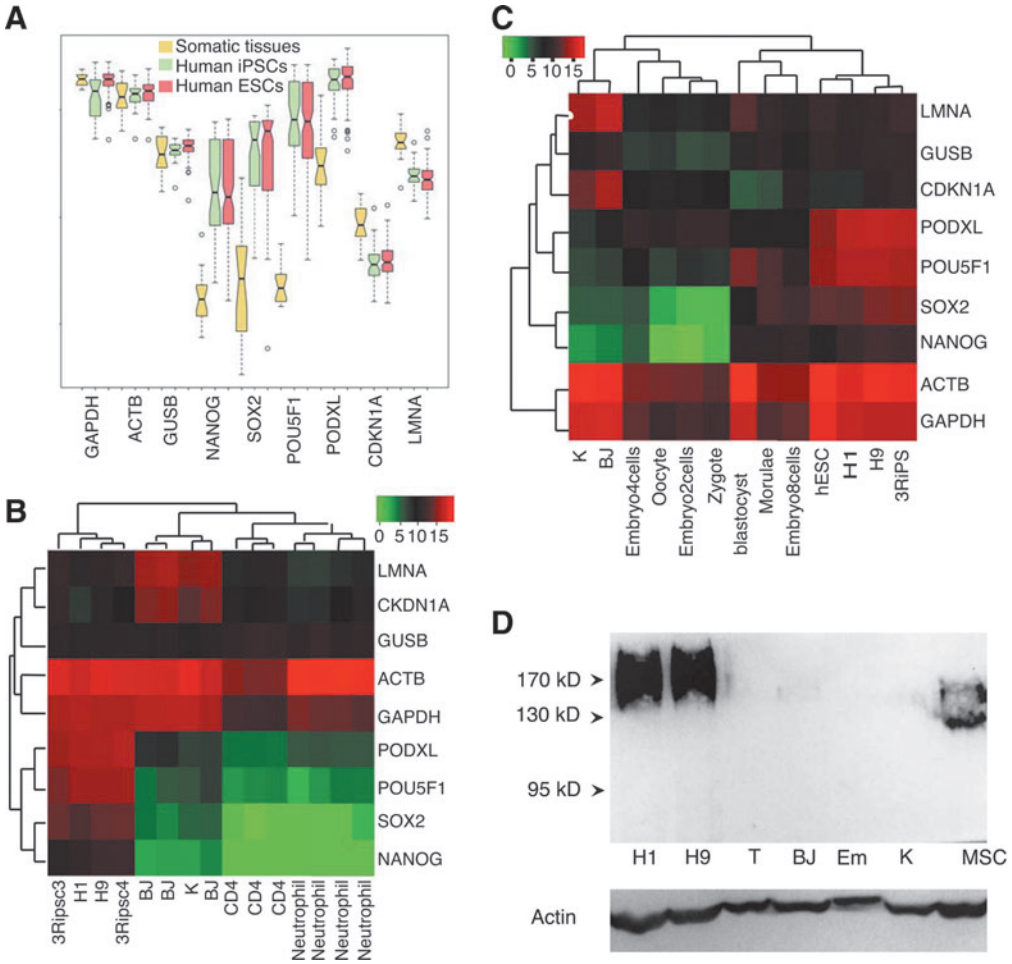

FIG. 1. *PODXL* is a pluripotent feature at transcription levels. **(A)** Boxplot demonstration of high *PODXL* expression in human pluripotent stem cells (hPSCs). Reanalysis of pluripotent microarray dataset GSE34200. **(B)** Normalized RNA-seq read counts of *PODXL* in hPSCs and somatic cells in comparison with pluripotent (*POU5F1*, *SOX2*, and *NANOG*), somatic (*LMNA* and *CDKN1A*), and housekeeping genes (*GUSB*, *ACTB*, and *GAPDH*). Based on dataset GSE66798, GSE71645, and GSE59528. **(C)** Heat map of RNA-seq data for *PODXL* expression along with selected genes in cells of early human embryos along with hPSC (hESC, H1, H9, and 3RiPSC2), BJ, and keratinocytes (K). Dataset GSE36552 and GSE66798. **(D)** Western blots of PODXL expression in hPSCs in comparison with human fibroblasts (BJ), T cells (T), keratinocytes (K), bone marrow stromal cells (MSC), and murine ESCs (Em). Antibody, 3D3. PODXL, podocalyxin-like protein.

expressions in hPSCs are even higher than that of the master pluripotent genes *OCT4* (*POU5F1*), *SOX2*, and *NANOG*. In somatic tissues, *PODXL* expression levels are significantly lower, but higher than that of the master pluripotent gene *NANOG* in hPSCs. This significant expression in somatic tissues can be explained by the high expression of *PODXL* in vascular endothelial cells, kidney podocytes, hematopoietic progenitors, some neural cells, platelets, and bone marrow stromal cells [45,46].

To avoid noise from the *PODXL*-expressing cells in tissue samples, we performed RNA-seq of several somatic cell lines and compared to the expressions in PSCs. Our RNA-seq dataset GSE66798 confirmed the array data in that *PODXL* has a higher expression in hPSCs than pluripotent genes *POU5F1*, *SOX2*, and *NANOG* (Fig. 1B). In human fibroblasts and keratinocytes, expression of *PODXL* is insignificant, and human CD4 and neutrophils do not express *PODXL* (Fig. 1B). One of the PODXL epitopes 3D3 represents the primary unmodified sequence. Therefore, 3D3 antibody can detect all glycoforms of PODXL. We then used 3D3 to compare the total protein expression levels between hPSCs and somatic cells. Our results show that PODXL is expressed in hPSCs but not in human fibroblasts, T cells, and keratinocytes, consistent with the mRNA expression pattern (Fig. 1D). In agreement with previous observations with TRA-1–81 antibodies (Fig. 2C), PODXL western bands are diffusive (Lanes H1 and H9 in Fig. 1D), indicating a spectrum of various post-translational modifications. 3D3 antibody does not recognize murine PODXL (lane Em in Fig. 1D; see below), which can serve as a negative control as well. As expected, human bone marrow stromal stem cells express PODXL but with lower molecular weights (Lane MSC in Fig. 1D) [46].

With the above observations, we wanted to know the expression status of *PODXL* in early human embryos. We reanalyzed the single-cell RNA-seq dataset GSE36552 of human embryos [47]. Interestingly, the expression of *OCT4 (POU5F)* correlates better with *PODXL* than with *NANOG*

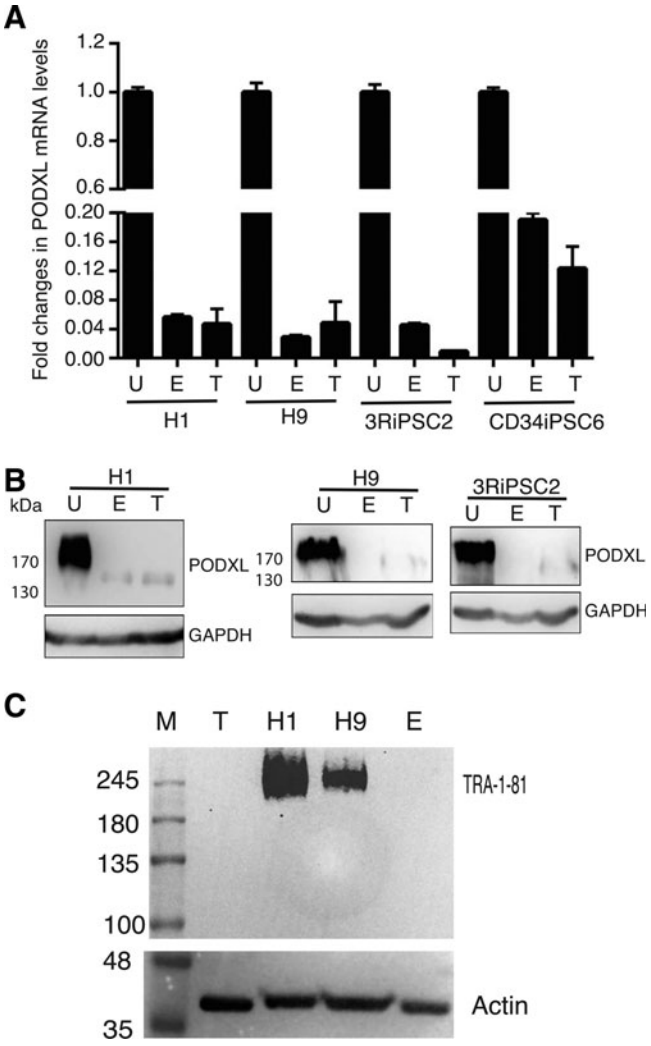

FIG. 2. PODXL is a differentiation marker. **(A)** Relative levels of PODXL upon differentiation. Results of RT-qPCR. **(B)**, Western blots of PODXL with the universal 3D3 antibody. **(C)** Western analysis of undifferentiated hPSCs (H1 and H9) and differentiated hPSCs, with the TRA-1-81 antibody, an established pluripotent epitope. M, protein marker. U, undifferentiated hPSCs; E, embryoid body-differentiated hPSCs; T, teratoma-differentiated hPSCs; H1 and H9, hESC lines H1 and H9; 3RiPSC2 and CD34iPSC6 are two HiPSC lines in our laboratory. RT-qPCR, reverse transcription-quantitative polymerase chain reaction.

and *SOX2* (Fig. 1C). But, *PODXL* has the highest expression in cells from oocyte up to 4-cell stages, while *POU5F1* peaks at morulae and blastocysts (Fig. 1C), and SOX2 and *NANOG* are not expressed from zygote to four-cell stage. At later stages, *PODXL* expression levels vary among cells (Supplementary Fig. S1). In summary, *PODXL* has a similar expression pattern in established pluripotent cells as those of the established pluripotent transcription factors OCT4, SOX2, and NANOG, and even has broader expression in early embryoes. *PODXL* transcription in hPSCs is comparable to the housekeeping gene beta actin, and significantly higher than its expression in somatic tissues. Its expression is high in early human embryos, and absent from the cultured fibroblasts and keratinocytes.

PODXL is downregulated upon differentiation of hPSCs

We next asked whether PODXL could be used as a pluripotent marker during the differentiation process, as its post-translational modification epitopes do. Two approaches were used. First, we performed in vitro EB-initiated differentiation and examined the expression levels by RT-qPCR and by western blots. *PODXL* RNAs were significantly reduced upon differentiation for two hESC lines (H1 and H9) (column E, left, Fig. 2A). Similar results were observed for two human iPSC lines established and characterized previously in our laboratory (column E, right, Fig. 2A). Western blot analyses with the universal PODXL antibody 3D3 confirmed the significant decrease of PODXL for both hESCs and HiPSCs upon differentiation (lane E, Fig. 2B). The molecular weight of PODXL in the differentiated cells is lower than those in undifferentiated cells, indicating the loss of post-translational modifications upon differentiations. The species of PODXL with lower molecular weight was previously observed in some somatic cells [16,37,38]. To further confirm the above observations, we used a second differentiation method, in vivo teratoma differentiation in immune compromised mice. Similar downregulation of PODXL were observed at both RNA and protein levels (T in Fig. 2A, B). As a control, we performed western analysis with the antibody TRA-1-81, as expected, we did not observe any band in teratoma and EB samples (Fig. 2C) while a diffused band was observed with both H1 and H9 undiffrentiated cells, indicating a loss of the TRA-1-81 epitope.

Residual PODXL$^+$ population remains after extended differentiation of hPSCs

Although PODXL is significantly downregulated both at mRNA and protein levels upon differentiation using both in vivo and in vitro protocols, there was residual PODXL expression based on western blot analysis. These residual expressions have two possibilities: (a) PODXL is downregulated in all cells; (b) Only some of cells are positive for PODXL upon differentiation. To distinguish these possibilities, we performed flow cytometry to examine PODXL expression in single cells. Our two distinct differentiation protocols stated above are efficient because there were no residual expressions for the two established pluripotent surface markers SSEA4 and TRA-1-60 in multiple hPSC lines analyzed (Fig. 3A and Supplementary Fig. S2). However, there are significant numbers of 3D3$^+$TRA-1-60$^-$SSEA4$^-$ cells after both EB and teratoma differentiations (Fig. 3A and Supplementary Fig. S2). This population was observed for both hESCs and HiPSCs. 3D3$^+$ cells ranged from 3.69% to 17.5% (Fig. 3A and Supplementary Fig. S2). We further conducted immunohistochemistry with 3D3 and OCT4 antibodies with teratoma sections. In agreement with flow cytometry data, we observed a 3D3$^+$ population, but did not detect any OCT4$^+$ cells (Fig. 3B). Based on these observations, it can be concluded that after prolonged differentiation the majority of cells are not expressing PODXL, but significant populations are still expressing PODXL at different levels.

KLF4 activates PODXL during early reprogramming

PODXL carrier epitopes are responsible for two well-known pluripotent surface markers TRA-1-60 and TRA-1-81, both of

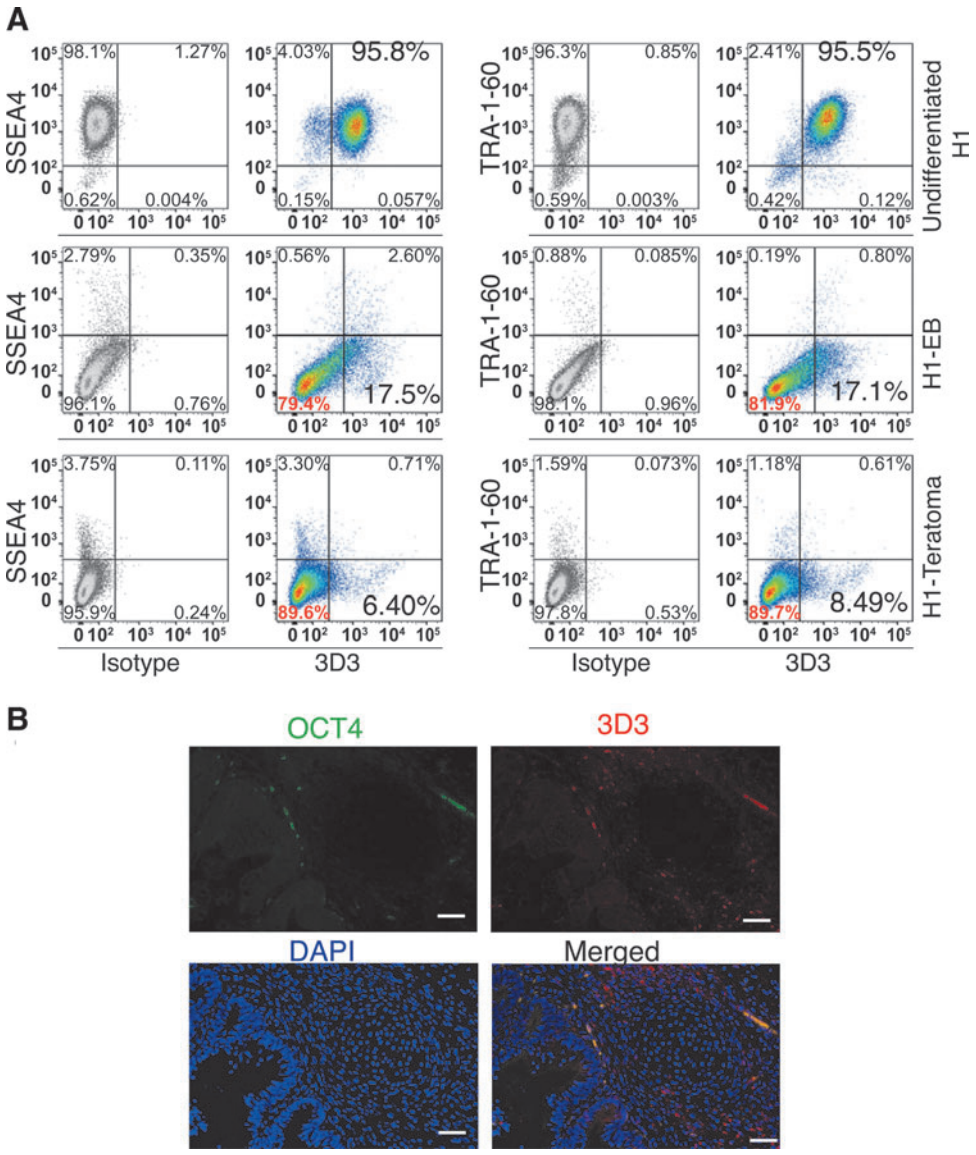

FIG. 3. The universal human PODXL antibody 3D3 identifies a residual population of $3D3^{+}TRA\text{-}1\text{-}60^{-}SSEA4^{-}$ cells. **(A)** Flow cytometry analysis of undifferentiated and differentiated human embryonic stem cells with 3D3 antibody. H1-EB, H1 hESCs differentiated with EB method; H1-teratoma, teratoma cells from H1. **(B)** Immunohistochemistry of H1-teratoma with antibody 3D3, and human OCT4 antibody. The *green* spots in OCT4 panel are background, which pick up 3D3 antibody also. Please note that there is no 3D3 signal in the central area, which is more differentiated cartilage (mesoderm). EB, embryoid body.

which are regarded as the most reliable markers for the generation of hiPSCs [48]. We were interested in how and when the *PODXL* gene is activated during human somatic cell reprogramming. We transduced human fibroblasts BJ cells with lentiviral Yamanaka factors (OCT4, SOX2, KLF4, and MYC), and performed RT-qPCR to test the expression of *PODXL* at 48 and 72 h post-transduction. Impressively, unlike the late emergence of TRA-1-60 and TRA-1-81 during reprogramming [48–50], *PODXL* expression levels were increased by >20-fold at both time points (Fig. 4A). Time point analyses showed that *PODXL* mRNA levels kept increasing up to day 21 (Fig. 4B). Western analyses with 3D3 antibody confirmed a robust and early activation of *PODXL* during reprogramming (Fig. 4C).

Next, we asked whether all four reprogramming factors are required for the early and robust activation of *PODXL* during reprogramming. As shown in Figure 4D, the combination of OSK demonstrated strong activation of *PODXL* at 48 and 72 h. Interestingly, removal of KLF4 dramatically affected the activation activity. Moreover, KLF4 alone activated *PODXL* more efficiently than OSK at both time points. Individually, the other three reprogramming factors alone showed little activation activities of *PODXL*. KLF4 activation of PODXL was confirmed by western blots (Fig. 4E) and immunocytochemistry (Fig. 4I) with 3D3 antibody. Regulation of *PODXL* by KLF4, but not the other reprogramming factors, was further substantiated with two luciferase reporter assays with upstream regulatory sequences of *PODXL* (Fig. 4F, G). Moreover, We also demonstrated that KLF4 directly bound to *PODXL* promoter using ChIP-qPCR (Fig. 4H). The transcription of *PODXL* has previously been reported to be positively regulated by WT1 and SP1 [51,52], but negatively by p53 [53]. In agreement with KLF4 and WT1 regulation of *PODXL*, WT1 and KLF4 are also critical for podocyte functions [54,55].

Mouse PODXL is a pluripotent marker

It is well known that TRA-1-60 and TRA-1-81 are unique surface markers for human PSCs that are not shared with mouse. However, TRA-1-60 and TRA-1-81 represent post-translational modification epitopes of PODXL. It is possible that only TRA-1-60 and TRA-1-81 epitopes are

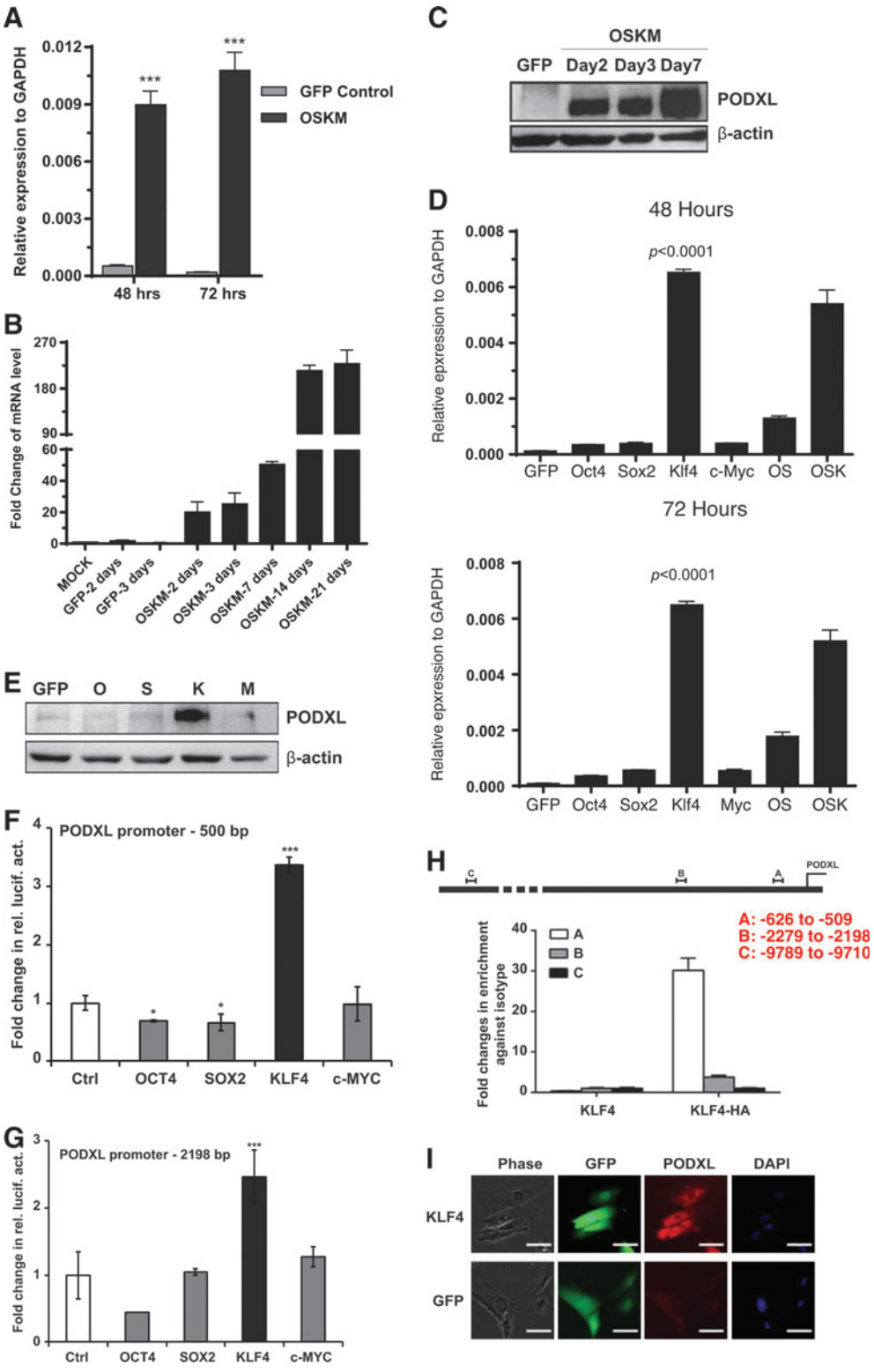

FIG. 4. KLF4 activates *PODXL* at an early time during reprogramming. **(A)** RT-qPCR analysis of *PODXL* in reprogramming cells. BJ cells were used. OSKM, OCT4, SOX2, KLF4, MYC. Average + SD, $n = 3$. **(B)** RT-qPCR measurement of *PODXL* levels in reprogramming BJ cells during the course of reprogramming. Average + SD, $n = 3$. **(C)** Western blots of PODXL with 3D3 antibody. BJ cells were transduced with OSKM viruses. Protein for GFP control was harvested on day 3 postviral transduction. **(D)** RT-qPCR analyses of PODXL levels in BJ cells transduced with viruses indicated. Time points checked are 48 and 72 h post-transduction. **(E)** Western analysis of BJ cells transduced with lentiviruses indicated. **(F, G)** Reporter assay of *PODXL* regulatory sequence in Hela cells transduced with viruses indicated. **(H)** qPCR analysis of chromatin DNA immunoprecipitated with PODXL antibody. **(I)** immunocytochemistry of BJ cells transduced with viruses indicated. $*p < 0.05$; $**p < 0.01$; $***p < 0.001$. SD, standard deviation.

unique to primate, but the carrier protein is also expressed in mouse PSCs. To test this hypothesis, we analyzed mouse ESC line E14 with a mouse PODXL antibody by flow cytometry. As previously known, E14 is positive for the mouse pluripotent surface marker SSEA1 (Fig. 5A), but negative for TRA-1-60 (Fig. 5A). But, PODXL is expressed in almost all mouse E14 cells (Fig. 5A). RT-qPCR further demonstrated that *PODXL* is highly expressed in E14 compared to mouse embryonic fibroblasts (MEF; compare the first and the last bar in Fig. 5C). We next examine whether KLF4 can also activate *PODXL* in mouse cells. We overexpressed human KLF4 in MEF. As in human cells, KLF4 but not OCT4 and SOX2 activated *PODXL* (Fig. 5C).

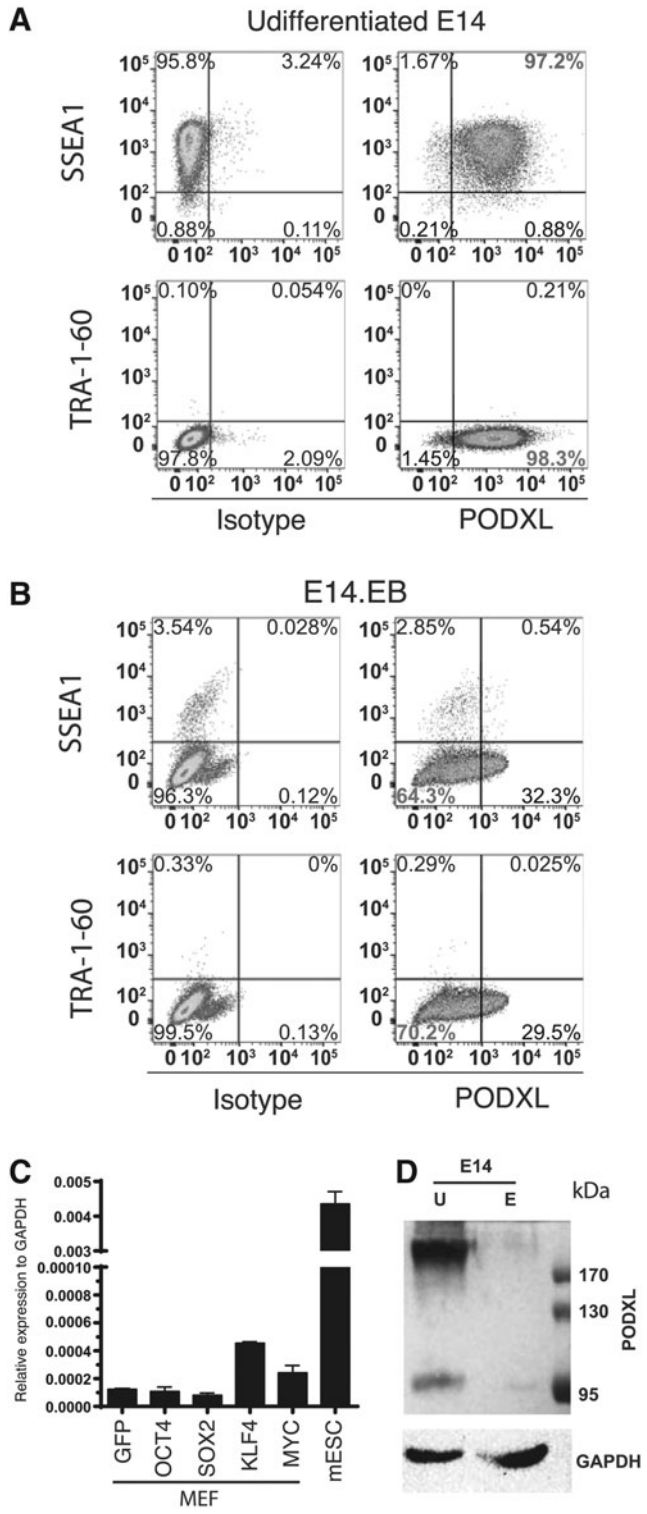

FIG. 5. PODXL is a mouse pluripotent marker. **(A)** Flow cytometry analysis of mouse ESC E14 with a mouse PODXL antibody. **(B)** Flow cytometry analysis of E14 cells differentiated by in vitro EB method with mouse PODXL antibody. **(C)** RT-qPCR analysis of PODXL in mESC, and mouse embryonic fibroblasts transduced with viruses indicated. **(D)** Western analysis of murine PODXL in undifferentiated E14 and EB differentiated E14.

We next asked whether PODXL is also a characteristic of mouse pluripotent cells as it is for human PSCs. To this end, we differentiated E14 using EB-FBS methods. Our protocol efficiently downregulated SSEA1, a mouse pluripotent surface marker (5B). Upon differentiation, most cells became $PODXL^-$. But higher percentage of $PODXL^+$ cells was observed relative to that observed upon differentiation of human PSCs. Nevertheless, the $PODXL^+$ cells expressed a lower level of PODXL based on the intensity of the fluorescence (Fig. 5B). We further conducted western analyses with murine PODXL antibody (Fig. 5D). Undifferentiated mouse embryonic stem cells express high levels of PODXL. Interestingly, a smaller band at around 98 kD was observed. Upon differentiation, intensity of both bands is significantly decreased to the levels slightly above background intensity.

3D3 is cytotoxic to human hPSCs

It is reported that one modification-dependent antibody mAb84 is cytotoxic to hPSCs [14]. This antibody is suggested to be useful in elimination of tumorigenic pluripotent cells in the future hPSC-derived transplants for cell therapy. Using annexin V-7AAD assay, we confirmed the cytotoxic nature of mAb84 when incubated with the detached hPSCs in test tubes for 45 min (right, Fig. 6A). However, when applied to cultured cells, mAb84 is not cytotoxic to hPSCs (right, Fig. 6B, Supplementary Figs. S3 and S4). We performed similar tests for 3D3; in contrast to mAb84, 3D3 is not cytotoxic when incubated for 45 min with detached hPSCs in test tubes (Fig. 6A). However, 3D3 is cytotoxic when added into hPSC culture for two days (Fig. 6B). We performed a growth curve evaluation for several PODXL antibodies including TRA-1-60, 3D3, and AF1658 (R&D) along with mouse and goat IgG controls, and another pluripotent marker SSEA4. Only 3D3 demonstrated cytotoxicity to hPSC. After exposure of human embryonic stem cell line H9 to 3D3 for 4 days, all hPSCs were dead but not other antibodies (Fig. 6D and Supplementary Fig. S3). We observed the same results with a human iPSC line (Fig. 6C). 3D3 cytotoxicity was observed with an additional embryonic stem cell line H1 (Supplementary Figs. S4 and S5). This cytotoxic effect of 3D3 was not seen with Hela cells, which express PODXL (Fig. 6E). Thus, the cytotoxic effect is specific for hPSCs and HiPSCs. mAb84 damages the cell membrane. It is possible that the broken cell membrane is responsible for the positivity for annexin V observed in 3D3-treated cells. To further confirm that 3D3 caused apoptosis, we performed western analysis with p21 antibody. We observed significant increase in p21 level in 3D3-treated H1 cells (Fig. 6F).

Discussion

Human embryonic stem cells are defined by a set of surface markers. One interesting fact is that many pluripotent marker antibodies were reported to recognize various epitopes of the same carrier protein PODXL [8,10,15], including TRA-1-60, TRA-1-81, GP200, GCTM2, and mAb84. These markers are expressed in hPSCs and embryonic carcinoma. Upon differentiation of hPSCs, these markers become lost. There has not been much emphasis paid to the carrier protein itself and the *PODXL* gene. In this

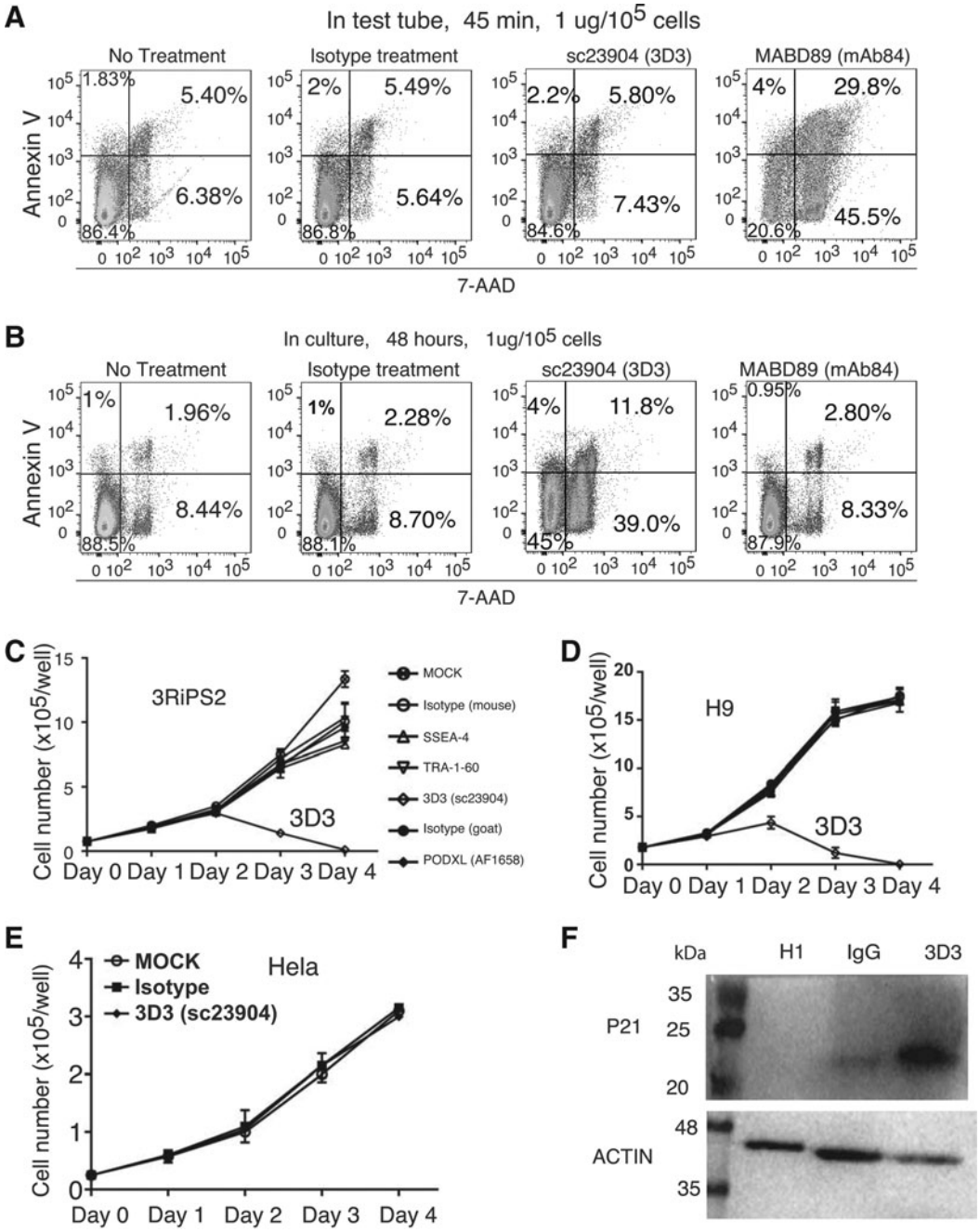

FIG. 6. 3D3 is cytotoxic to hPSCs. **(A)** Flow cytometry analyses of detached H9 treated in test tube for 45 min with antibodies indicated. **(B)** Flow cytometry analyses of H9 in culture in the presence of antibodies in media for 48 h. **(C–E)** growth curve of iPSCs **(C)**, H9 **(D)** and Hela cells **(E)** treated with antibodies indicated. **(F)** Western analysis of H1 hESCs treated with 3D3 with p21 antibody. Antibody treatments were performed for 48 h at 3 μg/mL. Fresh antibodies were added at 24 and 2 h before protein harvest with media change.

report, we demonstrated that a high level of mRNA of PODXL is also a feature of pluripotent stem cells. *PODXL* expression is extremely high in hPSCs, and comparable to that of housekeeping genes. It was higher than those of the master pluripotent transcription factors OCT4, SOX2, and NANOG. Upon differentiation, PODXL mRNA was downregulated to the basal levels. The modification-independent antibody 3D3 identifies a somatic PODXL species with lower apparent molecular weight and low intensity. Our results show that during differentiation, pluripotent cells lose modifications before downregulation of the gene.

It is well known that TRA-1-60 and TRA-1-81 are pluripotent surface markers specific to hPSCs not shared by mouse PSCs. In this study, we found that *Podxl* is expressed in mouse PSCs. This is confirmed by RT-qPCR analysis. This observation indicates that the carrier protein is conserved between rodent and human. Furthermore, in both species, KLF4 alone upregulated the transcription of *Podxl* gene.

One intrinsic feature of hPSCs is their ability to generate teratoma when injected into immunecompromised mice. This tumorigenic nature of PSCs has been a safety concern. hPSC-based cell therapy has entered clinical trials for the treatment of blindness, heart infarction, and spinal cord injury [56–60]. However, there is no safety regimen to eliminate the tumorigenic cells in hPSC-based transplants. Several suggestions have been made, including FACS or MACS sorting to separate therapeutic cells from the undifferentiated PSCs, the use of a suicide gene preintegrated into hPSCs, the use of cytotoxic antibodies, the use of cytotoxic small molecules, extended differentiation process, and individualization of cells [61–66]. However, even trace amount of incompletely differentiated cells may undergo a dedifferentiation process and give rise to tumors. This was reported for mouse $SSEA1^{+}OCT4^{-}$ cells [67] and for primate $SSEA4^{+}OCT4^{-}$ cells [63] in PSC-derived transplants.

In this study, we report a pluripotent cytotoxic activity of PODXL antibody 3D3. 3D3 antibody could be an invaluable means to eliminate the residual undifferentiated tumorigenic cells in hPSC-derived cells. 3D3 was raised against a PODXL fragment expressed in bacteria [16]. Therefore, this peptide is devoid of human post-translational modification. With this universal PODXL antibody, we identified a significant population of $3D3^{+}TRA\text{-}1\text{-}60^{-}SSEA4^{-}$ cells after extended differentiation. This population has never been revealed by the various modification-dependent pluripotent surface marker antibodies. It is reported that PODXL is involved in more than 10 different human malignancies [15,19–25], and it is also reported to have roles in metastasis and tumor invasion. With these in mind, there is an urgent need to investigate whether the $3D3^{+}TRA\text{-}1\text{-}60^{-}SSEA4^{-}$ cells are tumorigenic, and whether 3D3 antibody can be used to cleanse the tumorigenic cells in hPSC-derived transplants.

PODXL plays various roles including antiadhesion, adhesion, cell–matrix interaction, morphogenesis, cell migration, intracellular communication, and others [17,45,68]. The transcription regulation of *PODXL* is less clear. It is positively regulated by WT1 and SP1 [51,52], but negatively by p53 [53]. Here, we demonstrated that KLF4 is a new regulator of PODXL. PODXL plays a critical role in the development and functions of the kidney epithelium podocytes.

Acknowledgments

We thank Dr. Kevin Pawlik for his critical reading of our article. Data were deposited into GEO repository with an accession number GSE66798. This research is supported by a UAB faculty development grant and a stem cell seed grant from the Alabama Institute of Medicine (AIM) (AIMG1003).

Author Disclosure Statement

No competing financial interests exist.

References

1. Thomson JA, J Itskovitz-Eldor, SS Shapiro, MA Waknitz, JJ Swiergiel, VS Marshall and JM Jones. (1998). Embryonic stem cell lines derived from human blastocysts. Science 282:1145–1147.
2. Yu J, MA Vodyanik, K Smuga-Otto, J Antosiewicz-Bourget, JL Frane, S Tian, J Nie, GA Jonsdottir, V Ruotti, et al. (2007). Induced pluripotent stem cell lines derived from human somatic cells. Science 318:1917–1920.
3. Takahashi K, K Tanabe, M Ohnuki, M Narita, T Ichisaka, K Tomoda and S Yamanaka. (2007). Induction of pluripotent stem cells from adult human fibroblasts by defined factors. Cell 131:861–872.
4. Hu K. (2014). All roads lead to induced pluripotent stem cells: the technologies of iPSC generation. Stem Cells Dev 23:1285–1300.
5. Hu K. (2014). Vectorology and factor delivery in induced pluripotent stem cell reprogramming. Stem Cells Dev 23: 1301–1315.
6. Boyer LA, TI Lee, MF Cole, SE Johnstone, SS Levine, JP Zucker, MG Guenther, RM Kumar, HL Murray, et al. (2005). Core transcriptional regulatory circuitry in human embryonic stem cells. Cell 122:947–956.
7. Badcock G, C Pigott, J Goepel and PW Andrews. (1999). The human embryonal carcinoma marker antigen TRA-1-60 is a sialylated keratan sulfate proteoglycan. Cancer Res 59:4715–4719.
8. Schopperle WM and WC DeWolf. (2007). The TRA-1-60 and TRA-1-81 human pluripotent stem cell markers are expressed on podocalyxin in embryonal carcinoma. Stem cells 25:723–730.
9. Pera MF, MJ Blasco-Lafita, S Cooper, M Mason, J Mills and P Monaghan. (1988). Analysis of cell-differentiation lineage in human teratomas using new monoclonal antibodies to cytostructural antigens of embryonal carcinoma cells. Differentiation 39:139–149.
10. Natunen S, T Satomaa, V Pitkanen, H Salo, M Mikkola, J Natunen, T Otonkoski and L Valmu. (2011). The binding specificity of the marker antibodies Tra-1-60 and Tra-1-81 reveals a novel pluripotency-associated type 1 lactosamine epitope. Glycobiology 21:1125–1130.
11. Brimble SN, ES Sherrer, EW Uhl, E Wang, S Kelly, AH Merrill, Jr., AJ Robins and TC Schulz. (2007). The cell surface glycosphingolipids SSEA-3 and SSEA-4 are not essential for human ESC pluripotency. Stem cells 25:54–62.
12. Draper JS, C Pigott, JA Thomson and PW Andrews. (2002). Surface antigens of human embryonic stem cells: changes upon differentiation in culture. J Anat 200:249–258.
13. Tang C, AS Lee, JP Volkmer, D Sahoo, D Nag, AR Mosley, MA Inlay, R Ardehali, SL Chavez, et al. (2011). An antibody against SSEA-5 glycan on human pluripotent stem cells enables removal of teratoma-forming cells. Nat Biotechnol 29:829–834.
14. Tan HL, WJ Fong, EH Lee, M Yap and A Choo. (2009). mAb 84, a cytotoxic antibody that kills undifferentiated human embryonic stem cells via oncosis. Stem cells 27:1792–1801.
15. Schopperle WM, DB Kershaw and WC DeWolf. (2003). Human embryonal carcinoma tumor antigen, Gp200/GCTM-2, is podocalyxin. Biochem Biophys Res Commun 300: 285–290.
16. Kershaw DB, SG Beck, BL Wharram, JE Wiggins, M Goyal, PE Thomas and RC Wiggins. (1997). Molecular cloning and characterization of human podocalyxin-like protein. Orthologous relationship to rabbit PCLP1 and rat podocalyxin. J Biol Chem 272:15708–15714.
17. Nielsen JS and KM McNagny. (2009). The role of podocalyxin in health and disease. J Am Soc Nephrol 20:1669–1676.
18. Doyonnas R, DB Kershaw, C Duhme, H Merkens, S Chelliah, T Graf and KM McNagny. (2001). Anuria, om-

phalocele, and perinatal lethality in mice lacking the CD34-related protein podocalyxin. J Exp Med 194:13–27.
19. Sizemore S, M Cicek, N Sizemore, KP Ng and G Casey. (2007). Podocalyxin increases the aggressive phenotype of breast and prostate cancer cells in vitro through its interaction with ezrin. Cancer Res 67:6183–6191.
20. Casey G, PJ Neville, X Liu, SJ Plummer, MS Cicek, LM Krumroy, AP Curran, MR McGreevy, WJ Catalona, EA Klein and JS Witte. (2006). Podocalyxin variants and risk of prostate cancer and tumor aggressiveness. Hum Mol Genet 15:735–741.
21. Heukamp LC, HP Fischer, P Schirmacher, X Chen, K Breuhahn, C Nicolay, R Buttner and I Gutgemann. (2006). Podocalyxin-like protein 1 expression in primary hepatic tumours and tumour-like lesions. Histopathology 49:242–247.
22. Thomas SN, RL Schnaar and K Konstantopoulos. (2009). Podocalyxin-like protein is an E-/L-selectin ligand on colon carcinoma cells: comparative biochemical properties of selectin ligands in host and tumor cells. Am J Physiol Cell Physiol 296:C505–C513.
23. Somasiri A, JS Nielsen, N Makretsov, ML McCoy, L Prentice, CB Gilks, SK Chia, KA Gelmon, DB Kershaw, et al. (2004). Overexpression of the anti-adhesin podocalyxin is an independent predictor of breast cancer progression. Cancer Res 64:5068–5073.
24. Hayatsu N, MK Kaneko, K Mishima, R Nishikawa, M Matsutani, JE Price and Y Kato. (2008). Podocalyxin expression in malignant astrocytic tumors. Biochem Biophys Res Commun 374:394–398.
25. Larsson A, M Fridberg, A Gaber, B Nodin, P Leveen, G Jonsson, M Uhlen, H Birgisson and K Jirstrom. (2012). Validation of podocalyxin-like protein as a biomarker of poor prognosis in colorectal cancer. BMC Cancer 12:282.
26. Shao Z, R Zhang, A Khodadadi-Jamayran, B Chen, MR Crowley, MA Festok, DK Crossman, TM Townes and K Hu. (2016). The acetyllysine reader BRD3R promotes human nuclear reprogramming and regulates mitosis. Nat Commun 7:10869.
27. Kanduri K, S Tripathi, A Larjo, H Mannerstrom, U Ullah, R Lund, RD Hawkins, B Ren, H Lahdesmaki and R Lahesmaa. (2015). Identification of global regulators of T-helper cell lineage specification. Genome Med 7:122.
28. Chatterjee A, PA Stockwell, EJ Rodger, EJ Duncan, MF Parry, RJ Weeks and IM Morison. (2015). Genome-wide DNA methylation map of human neutrophils reveals widespread inter-individual epigenetic variation. Sci Rep 5: 17328.
29. Dobin A, CA Davis, F Schlesinger, J Drenkow, C Zaleski, S Jha, P Batut, M Chaisson and TR Gingeras. (2013). STAR: ultrafast universal RNA-seq aligner. Bioinformatics 29:15–21.
30. Anders S, PT Pyl and W Huber. (2015). HTSeq–a Python framework to work with high-throughput sequencing data. Bioinformatics 31:166–169.
31. Anders S and W Huber. (2010). Differential expression analysis for sequence count data. Genome Biol 11:R106.
32. Dillies MA, A Rau, J Aubert, C Hennequet-Antier, M Jeanmougin, N Servant, C Keime, G Marot, D Castel, et al. (2013). A comprehensive evaluation of normalization methods for Illumina high-throughput RNA sequencing data analysis. Brief Bioinform 14:671–683.
33. Quinlan AR and IM Hall. (2010). BEDTools: a flexible suite of utilities for comparing genomic features. Bioinformatics 26:841–842.
34. Kent WJ, AS Zweig, G Barber, AS Hinrichs and D Karolchik. (2010). BigWig and BigBed: enabling browsing of large distributed datasets. Bioinformatics 26:2204–2207.
35. Smyth GK. (2005). Limma: linear models for microarray data. In: *Bioinformatics and Computational Biology Solutions Using R and Bioconductor*. R Gentleman, V Carey, S Dudoit, R Irizarry and W Huber eds. Springer, New York, pp 397–420.
36. Choo AB, HL Tan, SN Ang, WJ Fong, A Chin, J Lo, L Zheng, H Hentze, RJ Philp, SK Oh and M Yap. (2008). Selection against undifferentiated human embryonic stem cells by a cytotoxic antibody recognizing podocalyxin-like protein-1. Stem Cells 26:1454–1463.
37. Wegner B, A Al-Momany, SC Kulak, K Kozlowski, M Obeidat, N Jahroudi, J Paes, M Berryman and BJ Ballermann. (2010). CLIC5A, a component of the ezrin-podocalyxin complex in glomeruli, is a determinant of podocyte integrity. Am J Physiol Renal Physiol 298:F1492–F1503.
38. Sassetti C, K Tangemann, MS Singer, DB Kershaw and SD Rosen. (1998). Identification of podocalyxin-like protein as a high endothelial venule ligand for L-selectin: parallels to CD34. J Exp Med 187:1965–1975.
39. Richards M, SP Tan, JH Tan, WK Chan and A Bongso. (2004). The transcriptome profile of human embryonic stem cells as defined by SAGE. Stem cells 22:51–64.
40. Zeng X, T Miura, Y Luo, B Bhattacharya, B Condie, J Chen, I Ginis, I Lyons, J Mejido, et al. (2004). Properties of pluripotent human embryonic stem cells BG01 and BG02. Stem Cells 22:292–312.
41. Bhattacharya B, T Miura, R Brandenberger, J Mejido, Y Luo, AX Yang, BH Joshi, I Ginis, RS Thies, et al. (2004). Gene expression in human embryonic stem cell lines: unique molecular signature. Blood 103:2956–2964.
42. Cai J, J Chen, Y Liu, T Miura, Y Luo, JF Loring, WJ Freed, MS Rao and X Zeng. (2006). Assessing self-renewal and differentiation in human embryonic stem cell lines. Stem Cells 24:516–530.
43. Brandenberger R, H Wei, S Zhang, S Lei, J Murage, GJ Fisk, Y Li, C Xu, R Fang, et al. (2004). Transcriptome characterization elucidates signaling networks that control human ES cell growth and differentiation. Nat Biotechnol 22:707–716.
44. Mallon BS, JG Chenoweth, KR Johnson, RS Hamilton, PJ Tesar, AS Yavatkar, LJ Tyson, K Park, KG Chen, YC Fann and RD McKay. (2013). StemCellDB: the human pluripotent stem cell database at the National Institutes of Health. Stem Cell Res 10:57–66.
45. Nielsen JS and KM McNagny. (2008). Novel functions of the CD34 family. J Cell Sci 121:3683–3692.
46. Lee MW, DS Kim, KH Yoo, HR Kim, IK Jang, JH Lee, SY Kim, MH Son, SH Lee, et al. (2013). Human bone marrow-derived mesenchymal stem cell gene expression patterns vary with culture conditions. Blood Res 48:107–114.
47. Yan L, M Yang, H Guo, L Yang, J Wu, R Li, P Liu, Y Lian, X Zheng, et al. (2013). Single-cell RNA-Seq profiling of human preimplantation embryos and embryonic stem cells. Nat Struct Mol Biol 20:1131–1139.
48. Chan EM, S Ratanasirintrawoot, IH Park, PD Manos, YH Loh, H Huo, JD Miller, O Hartung, J Rho, et al. (2009). Live cell imaging distinguishes bona fide human iPS cells from partially reprogrammed cells. Nat Biotechnol 27: 1033–1037.
49. Chou BK, P Mali, X Huang, Z Ye, SN Dowey, LM Resar, C Zou, YA Zhang, J Tong and L Cheng. (2011). Efficient

human iPS cell derivation by a non-integrating plasmid from blood cells with unique epigenetic and gene expression signatures. Cell Res 21:518–529.
50. Hockemeyer D, F Soldner, EG Cook, Q Gao, M Mitalipova and R Jaenisch. (2008). A drug-inducible system for direct reprogramming of human somatic cells to pluripotency. Cell Stem Cell 3:346–353.
51. Butta N, S Larrucea, S Alonso, RB Rodriguez, EG Arias-Salgado, MS Ayuso, C Gonzalez-Manchon and R Parrilla. (2006). Role of transcription factor Sp1 and CpG methylation on the regulation of the human podocalyxin gene promoter. BMC Mol Biol 7:17.
52. Palmer RE, A Kotsianti, B Cadman, T Boyd, W Gerald and DA Haber. (2001). WT1 regulates the expression of the major glomerular podocyte membrane protein Podocalyxin. Curr Biol 11:1805–1809.
53. Stanhope-Baker P, PM Kessler, W Li, ML Agarwal and BR Williams. (2004). The Wilms tumor suppressor-1 target gene podocalyxin is transcriptionally repressed by p53. J Biol Chem 279:33575–33585.
54. Guo JK, AL Menke, MC Gubler, AR Clarke, D Harrison, A Hammes, ND Hastie and A Schedl. (2002). WT1 is a key regulator of podocyte function: reduced expression levels cause crescentic glomerulonephritis and mesangial sclerosis. Hum Mol Genet 11:651–659.
55. Hayashi K, H Sasamura, M Nakamura, T Azegami, H Oguchi, Y Sakamaki and H Itoh. (2014). KLF4-dependent epigenetic remodeling modulates podocyte phenotypes and attenuates proteinuria. J Clin Invest 124:2523–2537.
56. Schwartz SD, CD Regillo, BL Lam, D Eliott, PJ Rosenfeld, NZ Gregori, JP Hubschman, JL Davis, G Heilwell, et al. (2015). Human embryonic stem cell-derived retinal pigment epithelium in patients with age-related macular degeneration and Stargardt's macular dystrophy: follow-up of two open-label phase 1/2 studies. Lancet 385:509–516.
57. Chapman AR and CC Scala. (2012). Evaluating the first-in-human clinical trial of a human embryonic stem cell-based therapy. Kennedy Inst Ethics J 22:243–261.
58. Menasche P, V Vanneaux, JR Fabreguettes, A Bel, L Tosca, S Garcia, V Bellamy, Y Farouz, J Pouly, et al. (2015). Towards a clinical use of human embryonic stem cell-derived cardiac progenitors: a translational experience. Eur Heart J 36:743–750.
59. Menasche P, V Vanneaux, A Hagege, A Bel, B Cholley, I Cacciapuoti, A Parouchev, N Benhamouda, G Tachdjian, et al. (2015). Human embryonic stem cell-derived cardiac progenitors for severe heart failure treatment: first clinical case report. Eur Heart J 36:2011–2017.
60. Sowden JC. (2014). ESC-derived retinal pigmented epithelial cell transplants in patients: so far, so good. Cell Stem Cell 15:537–538.
61. Fong CY, K Gauthaman and A Bongso. (2010). Teratomas from pluripotent stem cells: A clinical hurdle. J Cell Biochem 111:769–781.
62. Fong CY, GS Peh, K Gauthaman and A Bongso. (2009). Separation of SSEA-4 and TRA-1-60 labelled undifferentiated human embryonic stem cells from a heterogeneous cell population using magnetic-activated cell sorting (MACS) and fluorescence-activated cell sorting (FACS). Stem Cell Rev 5:72–80.
63. Shibata H, N Ageyama, Y Tanaka, Y Kishi, K Sasaki, S Nakamura, S Muramatsu, S Hayashi, Y Kitano, K Terao and Y Hanazono. (2006). Improved safety of hematopoietic transplantation with monkey embryonic stem cells in the allogeneic setting. Stem Cells 24:1450–1457.
64. Tateno H, Y Onuma, Y Ito, F Minoshima, S Saito, M Shimizu, Y Aiki, M Asashima and J Hirabayashi. (2015). Elimination of tumorigenic human pluripotent stem cells by a recombinant lectin-toxin fusion protein. Stem Cell Reports 4:811–820.
65. Richards M, CW Phoon, GT Goh, EK Seng, XM Guo, CM Tan, WK Chan and JM Lee. (2014). A new class of pluripotent stem cell cytotoxic small molecules. PLoS One 9:e85039.
66. Vazquez-Martin A, S Cufi, E Lopez-Bonet, B Corominas-Faja, C Oliveras-Ferraros, B Martin-Castillo and JA Menendez. (2012). Metformin limits the tumourigenicity of iPS cells without affecting their pluripotency. Sci Rep 2:964.
67. Fujikawa T, SH Oh, L Pi, HM Hatch, T Shupe and BE Petersen. (2005). Teratoma formation leads to failure of treatment for type I diabetes using embryonic stem cell-derived insulin-producing cells. Am J Pathol 166:1781–1791.
68. Larrucea S, N Butta, EG Arias-Salgado, S Alonso-Martin, MS Ayuso and R Parrilla. (2008). Expression of podocalyxin enhances the adherence, migration, and intercellular communication of cells. Exp Cell Res 314: 2004–2015.

Address correspondence to:
Dr. Kejin HU
Stem Cell Institute, Department of Biochemistry and Molecular Genetics
University of Alabama at Birmingham
Birmingham, AL 35294-0024

E-mail: kejinhu@uab.edu

Received for publication October 5, 2015
Accepted after revision February 16, 2016
Prepublished on Liebert Instant Online February 17, 2016